Registered in Germany **Europa Revue Journal**
ISSN: 1862-6564 **Vol. 6 No. 6 (2026) Published June 30, 2026**

DEVELOPMENT OF AN OPTIMAL ENGINE CONTROL MODEL FOR A COMPRESSOR SYSTEM

Zakirova Dilnoza Nematillayevna

Associate Professor, Department of Energy Engineering, Namangan State Technical University

Abstract

The article *considers mathematical and simulation models of starting an asynchronous motor of a compressor unit . The main attention is paid to the starting processes of an asynchronous motor. It is proposed to replace the traditional method of drive control with frequency control. On this basis, simulation of the operation of a frequency-controlled drive system under various operating conditions was carried out, and on their basis, optimal control conditions for a three-phase motor were proposed.*

Keywords

engine control model, compressor installation, sorter ramp, engine control, frequency control, output power control, compressor engine, engine start-up.

the compressor unit (K Q) is to continuously supply the devices included in the technological process with compressed air. This mode of operation of K Q prevents the mechanisms from stopping without reducing their speed, which leads to a large consumption of electricity for processing one composition. At the same time, interruptions in engine operation during periods of inactivity at the station have negative consequences, since the windings of the machine heat up significantly when it is next started.

These two problems are caused by the compressor unit's engines. is associated with the lack of control of rotor torque and speed [1]. It is known that the lack of control of these parameters significantly worsens the starting characteristics, shortens the life and complicates the starting process of synchronous and asynchronous motors [2].

However, advances in modern power electronics and microprocessor technology help to solve these problems. Modern frequency and vector control algorithms provide

the smoothest operating characteristics of synchronous and asynchronous machines of any power [3].

The main task of such algorithms is to ensure smooth start/stop of the electric drive, control of the rotor speed and electromagnetic torque over a wide range.

Solving these issues allows optimizing the operating modes of the K Q engine, significantly extending its service life, and reducing the overall energy consumption of the system [2].

It is known that to develop a frequency-based control system - scalar or vector - it is necessary to take into account the application characteristics, type, and brand of the engine [4].

Therefore, in this article, the following should be done:

Analysis of the electromechanical characteristics of the 5AH315A2C asynchronous motor used on the Donetsk road;

Determine the motor frequency control law and the method of generating the control signal;

Building a mathematical and computer model representing the operation of the motor under frequency control;

Comparative analysis of the existing and developed control model for compressed air efficiency management in K Q ;

Determining the optimal mode for starting a motor under load under frequency control .

It is known that a three-phase AC motor is a fully controlled machine if its electromagnetic torque can be controlled [5]. Therefore, the mathematical model of motor control uses an expression related to this quantity.

Let's look at the equation describing the operation of a three-phase AC motor:

$$M = \frac{pm_1 U_1^2 \frac{r_2}{s}}{\omega_1 \left[\left(r_1 + \frac{r\prime_2}{s}\right)^2 + (x_1 + x\prime_2)^2\right]} \qquad (1)$$

Here:

p– the number of stator pole pairs;

m_1– the number of phases feeding the stator;

U_1– supply voltage of the stator winding.

r_1- active resistance of the stator winding;

r'_2- equivalent active resistance of the rotor winding;

x_1- inductive resistance of the stator winding;

x'_2- equivalent inductive resistance of the rotor winding;

s– slide coefficient $s = \frac{\omega_1 - \omega}{\omega_1}$;

ω_1 – synchronous frequency of the motor $\omega_1 = \frac{60f}{p(1-s)}$;

ω– rotor rotation speed.

(1) As can be seen from the equation, the torque M is the stator voltage $U_1$and $f_1$frequency. Typically, in a compressor installation , these values are constant and are 50 Hz and 380 V, respectively. Therefore, the rotor rotates with a constant speed and torque. As a result, the motor is subjected to large overloads during start-up or load changes.

However, for a frequency control system (FCS), these values are variable and can be adjusted to any operating conditions as needed [2]. This is done by generating a pulse-width modulated (PWM) control signal that reproduces a sinusoidal voltage of a specified amplitude and frequency with maximum accuracy.

Let's take a closer look at this signal. Some restrictions are imposed on it:

- The amplitude of the signal must change symmetrically with respect to zero potential (bipolar CHIM signal);

- The modulation frequency must not be lower than the specified frequency [6];

- The modulation frequency must not exceed the specified maximum frequency.

These constraints allow us **to choose an algorithm for generating a CHIM (clock total pulse modulation) signal** . One such algorithm is the implementation of **a precise phase CHIM** . The shape of such a signal is shown **in Figure 1** , and its **mathematical model is (2) expressed in appearance** .

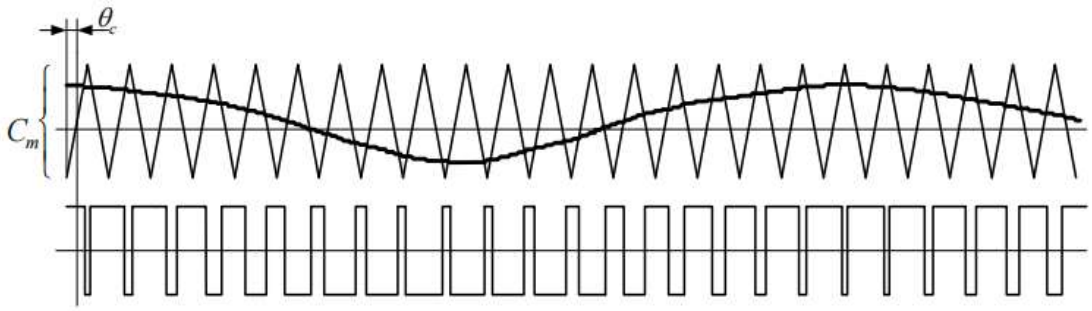


Figure 1. Timing diagram of a control pulse-width modulated (CHIM) signal

$$\begin{cases} u_{pwm}(t) = \frac{M}{2}\cos(\omega_1 t + \theta_1) + \sum_{m=1}^{+\infty} \frac{2}{m\pi} J_0\left(\frac{m\pi M}{2}\right) \sin\frac{m\pi}{2} \cos\left(m(\omega_c t + \theta_c)\right) + \\ + \sum_{m=1}^{+\infty} \sum_{n=\pm 1}^{\pm\infty} \frac{2}{m\pi} J_n\left(\frac{m\pi M}{2}\right) \sin\frac{(m+n)\pi}{2} \cos\left(m(\omega_c t + \theta_c) + n(\omega_1 t + \theta_1)\right) \\ U_1 \in [-U_{1m};\ +U_{1m}]; \\ \omega_{VT} > \omega_c > \omega_K. \end{cases}, \quad (2)$$

Here: $M = \frac{2U_1}{c_m}$ modulation index;

J_n- Bessel function of the first kind $J_n(z) = \frac{j^{-n}}{\pi}\int_0^{2\pi} e^{jz\cos\theta} e^{jn} d\theta$;

ω_s- angular frequency of the ball signal $\omega_s = 2\pi f_s$;

ω_1- fundamental frequency of the ball signal $\omega_1 = 2\pi f_1$;

θ_s- the initial phase of the ball signal;

θ_1- initial phase of the main signal;

U_1- amplitude of the main sinusoidal voltage;

c_m- gear signal amplitude;

U_{1m}- main signal amplitude;

ω_{VT}, ω_K- the limits of permissible corner frequencies for power switches and the frequencies specified in the Kotelnikov manual.

(2) The first component in the equation is the fundamental signal, which determines the location of the output signal relative to zero potential [7]. At the same time, it also acts as a function that determines the voltage shape at the inverter output.

(2) The second and third components of the equation are the harmonic series of the CHIM signal, expressed in the form of Fourier functions.

Now (2) We write the equation for a three-phase system.

$$\begin{cases} u_{pwmA}(t) = \frac{M}{2}\cos(\omega_1 t) + \sum_{m=1}^{+\infty}\frac{2}{m\pi}J_0\left(\frac{m\pi M}{2}\right)\sin\frac{m\pi}{2}\cos\left(m(\omega_c t+\theta_c)\right)+ \\ \quad + \sum_{m=1}^{+\infty}\sum_{n=\pm1}^{\pm\infty}\frac{2}{m\pi}J_n\left(\frac{m\pi M}{2}\right)\sin\frac{(m+n)\pi}{2}\cos\left(m(\omega_c t+\theta_c)+n(\omega_1 t)\right) \\ u_{pwmB}(t) = \frac{M}{2}\cos(\omega_1 t+120) + \sum_{m=1}^{+\infty}\frac{2}{m\pi}J_0\left(\frac{m\pi M}{2}\right)\sin\frac{m\pi}{2}\cos\left(m(\omega_c t+\theta_c)\right)+ \\ \quad + \sum_{m=1}^{+\infty}\sum_{n=\pm1}^{\pm\infty}\frac{2}{m\pi}J_n\left(\frac{m\pi M}{2}\right)\sin\frac{(m+n)\pi}{2}\cos\left(m(\omega_c t+\theta_c)+n(\omega_1 t+120)\right) \\ u_{pwmC}(t) = \frac{M}{2}\cos(\omega_1 t+240) + \sum_{m=1}^{+\infty}\frac{2}{m\pi}J_0\left(\frac{m\pi M}{2}\right)\sin\frac{m\pi}{2}\cos\left(m(\omega_c t+\theta_c)\right)+ \\ \quad + \sum_{m=1}^{+\infty}\sum_{n=\pm1}^{\pm\infty}\frac{2}{m\pi}J_n\left(\frac{m\pi M}{2}\right)\sin\frac{(m+n)\pi}{2}\cos\left(m(\omega_c t+\theta_c)+n(\omega_1 t+240)\right) \end{cases} . \quad (3)$$

(3) The system of equations applies to all asynchronous and synchronous three-phase machines. However, this model has some disadvantages for frequency-controlled drives. When the supply frequency changes, the distribution of rotor torques is not uniform across the entire frequency range [4]. At the same time, the current increases significantly due to the reduction in reactive resistance, which can lead to overheating and damage to the stator windings.

Therefore, for the correct and safe operation of the three-phase control system model, the control algorithms must be considered within a certain frequency range.

K Q system, if the load torque does not change over a large range, the optimal frequency control law is selected, provided that the torque is kept constant in the frequency range from 5 to 50 Hz.

$$\frac{U_1}{U\prime_1} = \frac{f_1}{f\prime_1}\sqrt{\frac{M_1}{M\prime_1}} \qquad (4)$$

Here:

$\frac{U_1}{U\prime_1}$– the ratio between the stator voltage before the frequency change and the stator voltage after the frequency change;

f_1– supply voltage frequency;

f'_1– the changed value of the supply voltage frequency;

$\frac{M_1}{M\prime_1}$– the ratio between the rotor torque before the voltage frequency change and the rotor torque after the change.

According to this law, the rotor torque is constant over the control frequency range [6]. If the frequency exceeds 50 Hz, the electromagnetic torque of the motor decreases significantly, which can lead to its complete standstill at some rotor loads.

Also, most K Q mechanisms are designed to operate at industrial frequencies. In this case, an increase in rotor speed can lead to clutch failure, severe friction, and wear of mechanical parts.

When the control frequencies are below 5 Hz, the mechanical characteristics of the asynchronous motor (AD) decrease, the critical torque point is located below the *X* axis, and thus the limits of the torque operating zone at the nominal K Q operation are reduced.

Taking into account these conditions and the need to maintain a constant rotor torque, (4) The equation is expressed as follows:

$$\frac{U_1}{f_1} = \frac{U'_1}{f'_1} = M = const \qquad (5)$$

At the same time, the AD family of mechanical properties looks like the one presented in Figure 2.

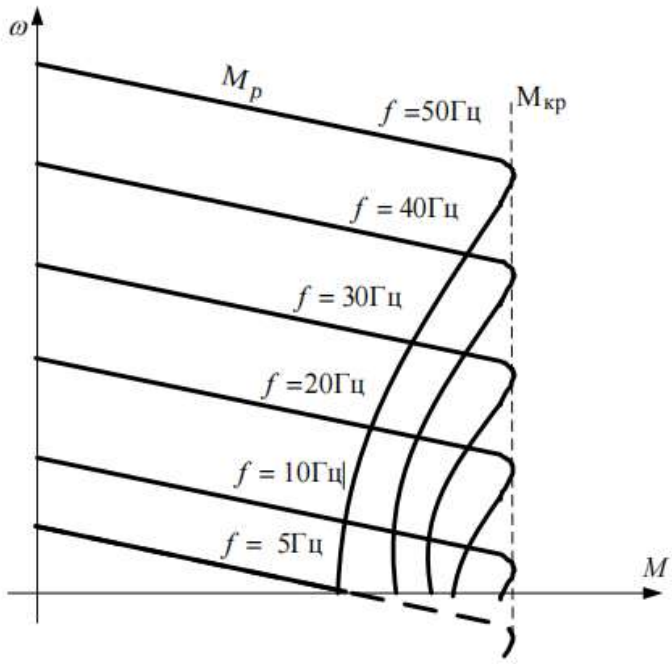


Figure 2. AD mechanical characteristic according to the frequency control law

According to condition (5), we plot the correspondence of the actual values of the phase voltage and its frequency in a tabular form (Table 1) . Also, a proportionality coefficient is introduced in the control model, which ensures the equilibrium state of the rotor torque, with a frequency range from 5 to 50 Hz.

$$K=\frac{U_{1nom}}{f_{1nom}}=\frac{380}{50}=7.6 \qquad (6)$$

1-Table

U_d, V	38	76	152	228	304	380	380	380
f, Hz	5	10	20	30	40	50	60	70
K	7.6	7.6	7.6	7.6	7.6	7.6	6.3	5.3

1 , frequencies outside the motor control range have been intentionally included. This is done to demonstrate the mechanical characteristics of the AD when the control frequency is increased to 70 Hz (Figure 3).

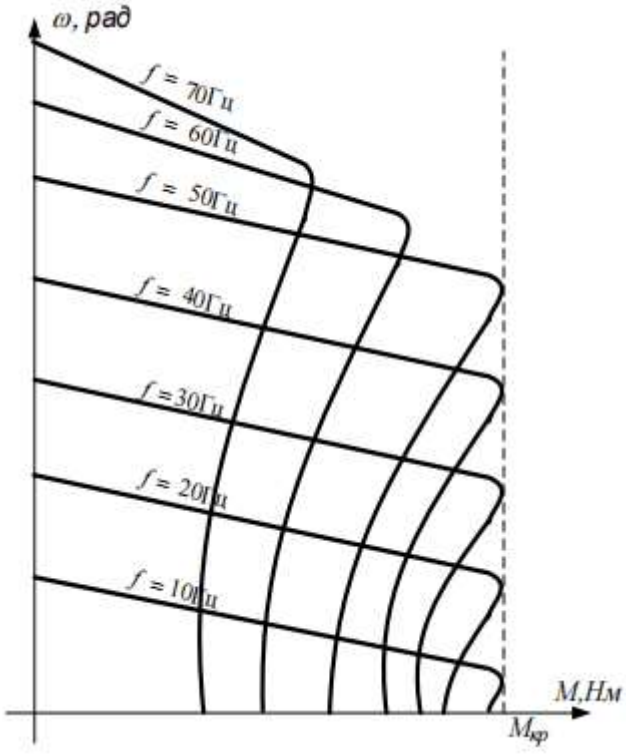


Figure 3. Frequency control range of the 5AH315A2C engine $f\epsilon[5;70]$mechanical properties in

the optimal limit of AD rotor speed control for K Q is the frequency range $f\epsilon[5;50](7)$ The equation is a mathematical model of motor frequency control with a precise phase CHIM signal generation algorithm, which ensures constant electromagnetic torque in the frequency range from 5 to 50 Hz.

$$\begin{cases} u_{pwmA}(t) = K\frac{M}{2}\cos(\omega_1 t) + \sum_{m=1}^{+\infty}\frac{2}{m\pi}J_0\left(K\frac{m\pi M}{2}\right)\sin\frac{m\pi}{2}\cos\left(m(\omega_c t+\theta_c)\right) + \\ \quad + \sum_{m=1}^{+\infty}\sum_{n=\pm1}^{\pm\infty}\frac{2}{m\pi}J_n\left(K\frac{m\pi M}{2}\right)\sin\frac{(m+n)\pi}{2}\cos\left(m(\omega_c t+\theta_c)+n(\omega_1 t)\right) \\ u_{pwmB}(t) = K\frac{M}{2}\cos(\omega_1 t+120) + \sum_{m=1}^{+\infty}\frac{2}{m\pi}J_0\left(K\frac{m\pi M}{2}\right)\sin\frac{m\pi}{2}\cos\left(m(\omega_c t+\theta_c)\right) + \\ \quad + \sum_{m=1}^{+\infty}\sum_{n=\pm1}^{\pm\infty}\frac{2}{m\pi}J_n\left(K\frac{m\pi M}{2}\right)\sin\frac{(m+n)\pi}{2}\cos\left(m(\omega_c t+\theta_c)+n(\omega_1 t+120)\right) \\ u_{pwmC}(t) = K\frac{M}{2}\cos(\omega_1 t+240) + \sum_{m=1}^{+\infty}\frac{2}{m\pi}J_0\left(K\frac{m\pi M}{2}\right)\sin\frac{m\pi}{2}\cos\left(m(\omega_c t+\theta_c)\right) + \\ \quad + \sum_{m=1}^{+\infty}\sum_{n=\pm1}^{\pm\infty}\frac{2}{m\pi}J_n\left(K\frac{m\pi M}{2}\right)\sin\frac{(m+n)\pi}{2}\cos\left(m(\omega_c t+\theta_c)+n(\omega_1 t+240)\right) \\ \omega_1 = 2\pi f \\ f \in [5;50] \end{cases} \quad (7)$$

Using the Simulink software environment, we develop and analyze a computer model based on this system of equations. Such a model includes the following structural blocks (Figure 4):

- source;
- Three-phase transistor bridge (IGBT-based inverter);
- Output LC filter;
- Asynchronous motor (brand 5AH315A2C);
-CHIM signal generator.

Parameters of the 5AH315A2C engine [9]:

- Power: 200 kW; frequency control — scalar, with constant torque;
- Nominal stator voltage: 380 V, three-phase;
- Nominal frequency: 50 Hz;
- Nominal rotor speed: 1500 rpm;
- Nominal phase current: 373 A;
- Stator resistance: 0.021 Ω, stator winding inductance: 0.000155 H;
- Rotor resistance: 0.017 Ω, rotor winding inductance: 0.000155 H;
- Mutual inductance between rotor and stator: 0.00755 H;
- Moment of inertia: 2.1 kg m²;
- Friction force: 0.05668 N;
- Overload coefficient: 2.1;
- Number of poles: 2;

- Initial slide coefficient: 1;

- Initial rotor speed: 0 rpm.

Considering this, (3) We rewrite the system of equations.

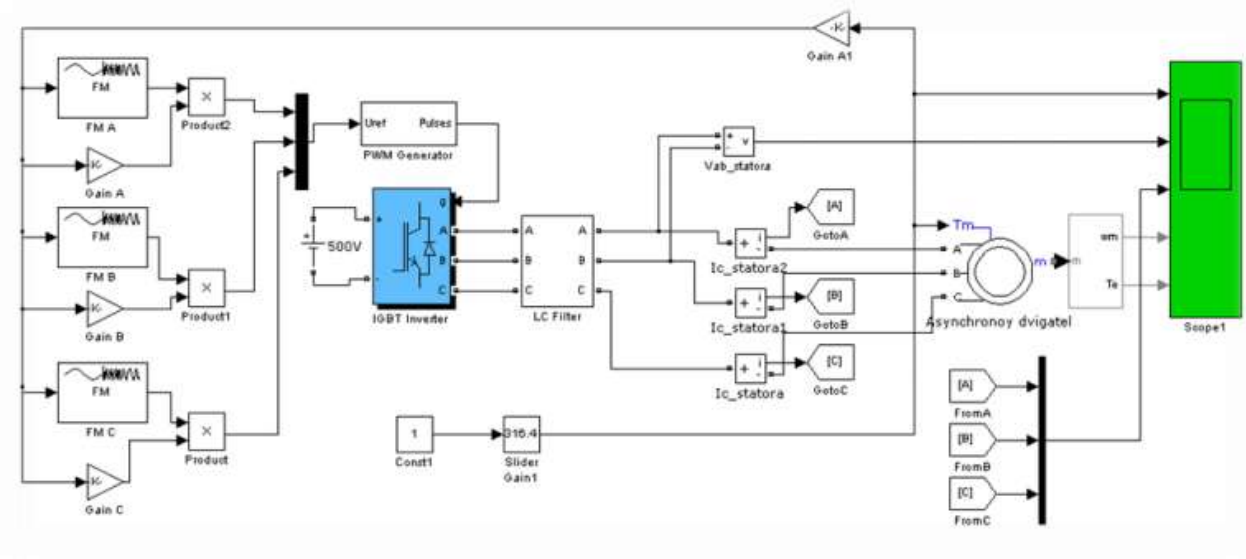


Figure 4. Computer model of the automatic control system of the compressor drive motor

The 5AH315A2C motor is powered by a three-phase inverter , which operates via a control input (7) coming from the module (left part of the diagram).

The main factor influencing the node that generates this law is the pressure level in the air line, which is converted into a proportional electrical signal (top part of the diagram).

In general terms, such a model is described by the following expression:

$\omega = f(p(t))$ (8)

here: $p(t)$– current pressure level in the air main, MPa;

ω – angular velocity of the driver motor rotor, rad/s.

Let's look at the system in action (Figure 5). Before starting, K has a non-zero pressure level in the air line Q. This is sufficient to create a load resistance of 70 Nm at start-up.

The AD soft start algorithm prevents large current and torque jumps. As the rotor speed increases linearly, the compressed air pressure also increases. When the

pressure reaches a threshold level of approximately 8.6 atm (engine torque 637 Nm), the system reduces the drive's operating intensity.

In 2 seconds (Fig. 5), 3 discharges are made through the air retarder. The air system has high inertia due to the collector, so the pressure level decreases slowly and smoothly, without transients. Then the pressure is quickly restored and maintained at the required level.

As can be seen from the graph, the pressure recovery rate in the mains is higher than the compressed air consumption. To analyze the starting modes at different control frequencies, a family of mechanical characteristics of the engine is considered (Fig. 6). At the same time, we determine the maximum rotor load.

The electromagnetic torque that a motor can produce is calculated by the following formula:

$$M_{EM} = \frac{P}{\omega_1}$$

here: P – electric power of the engine, W;

ω_1– synchronous angular velocity of the engine, rad/s.

The load torque must not exceed the following value, otherwise the engine will fail or stop. Therefore, for the 5AH315A2C engine, M_{EM} =M $_{max}$ is taken as =637 Nm.

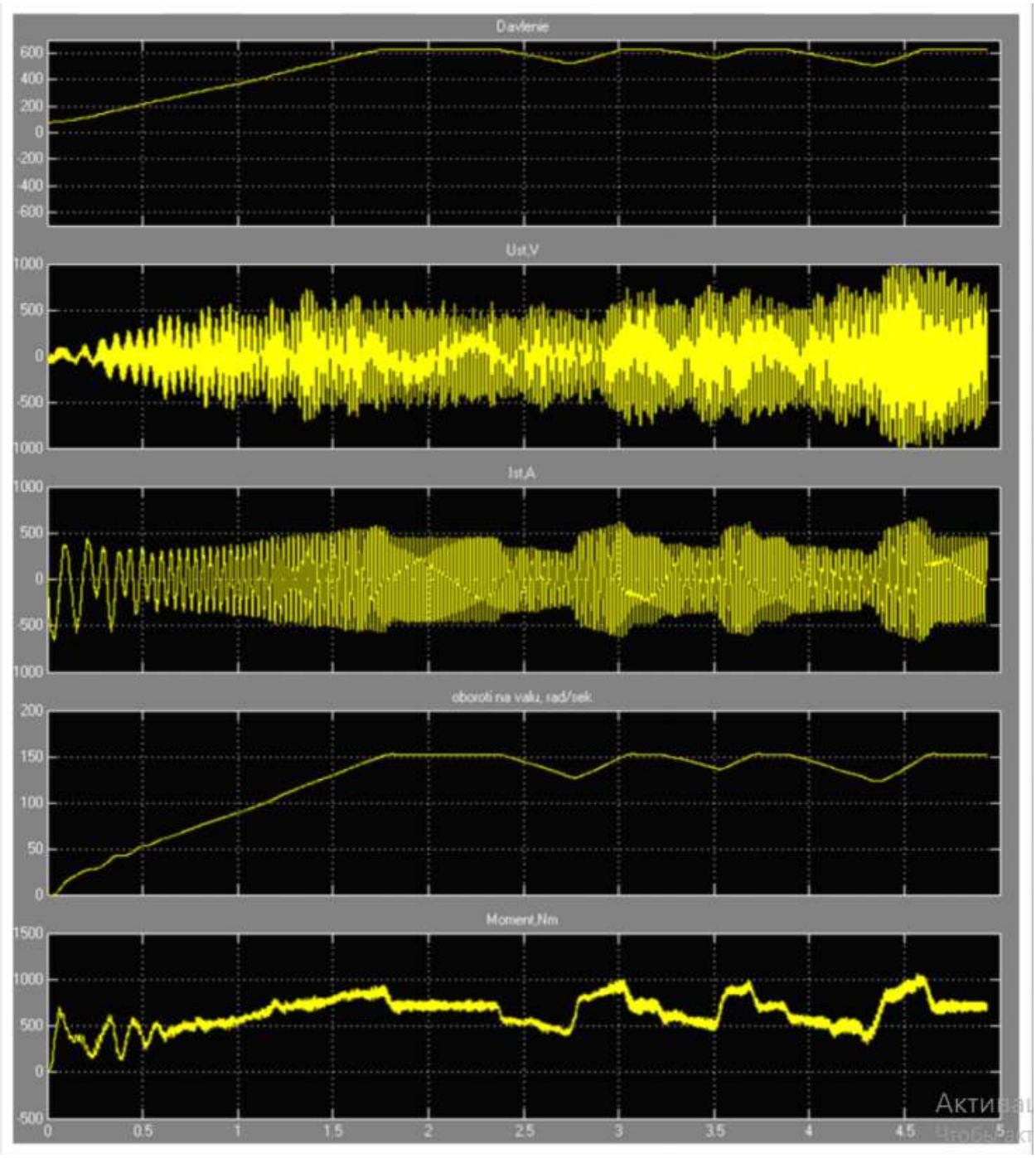


Figure 5. Timing diagrams for starting and controlling the compressor unit engine

Frequency control of AD (CHBT) Let's look at the mechanical properties of .

The mechanical characteristics are designed to provide a soft start of the motor and a linear acceleration of the rotor, which continues from 1 Hz to the operating frequency. This algorithm allows to minimize jumps in starting currents and rotor torque.

As can be seen from the figure, all characteristics have sufficient rigidity, which is typical for a conventional AD starting from a three-phase industrial network. Also, the stable operating limit has a reserve against overload: At frequencies of 20, 30, 40, 50 Hz – 2.2–2.5 times; At a frequency of 10 Hz – 1.5 times.

But the last diagram shows that for this engine there is no overload reserve at maximum load at a control frequency of 5 Hz. Therefore, with a suitable pressure level in the air line, when generating a 5 Hz control signal, the AD should switch to a “soft” shutdown mode.

from Figures 4 and 5 , the main advantage of the motor over the existing control system is the ability to operate without sharp jumps in current and electromagnetic torque, since the current is regulated through "soft" control.

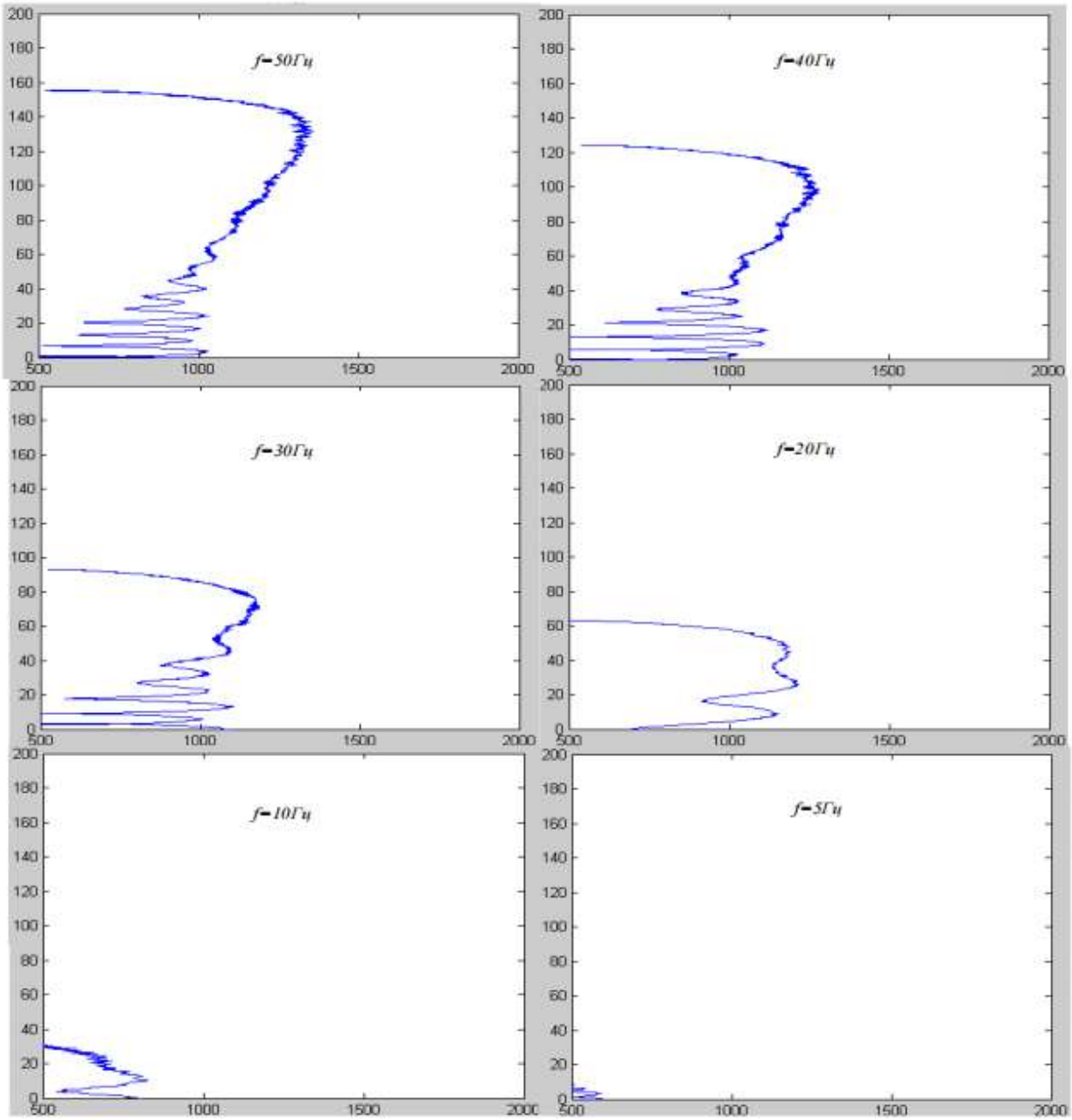


Figure 6. Mechanical characteristics of the 5AH315A2C engine at different control frequencies.

For comparison, the starting process of K Q motors was studied with a conventional automatic control system and a frequency control system. For this, experiments were conducted on two systems, both of which operated with a load of 300 Nm (Figure 7).

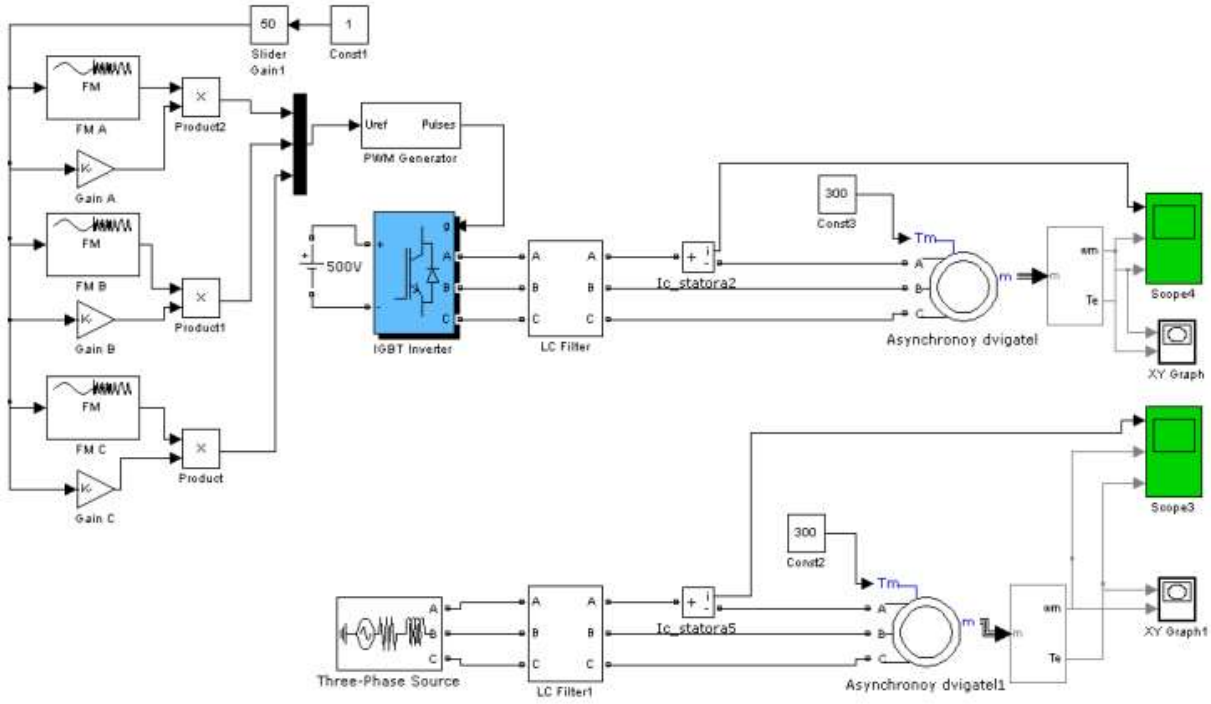


Figure 7. Comparative experience of the operation of two compressor unit engine control systems.

Figure 8 presents comparative diagrams of the launches.

The left part of the diagram is the launch of K Q with CHBT (Figure 7, top model);

The right part is the traditional system (Figure 8, bottom model).

As can be seen from the diagrams, the frequency control system enters the stable mode with a small delay when started. At the same time, the amplitude of the currents and torques during the transition period is half as small.

K Q is the same, that is, it operates at a frequency of 50 Hz and a voltage of 380 V.

Table 2. Comparison of the startup characteristics of CHBT and conventional K Q control systems.

KU with frequency control	KU with traditional management
Load torque, Nm	300
Maximum current, A	1820

Also, the analysis of the specified characteristics made it possible to determine the dependence of the starting currents and torques of the engine, as well as the duration of the transition process on the rotor acceleration. This makes it possible to optimize the process of safe starting of the AD under load.

Critical torque, Nm	2050
Minimum electromagnetic torque, Nm	0
Duration of the transition process, s	0.3

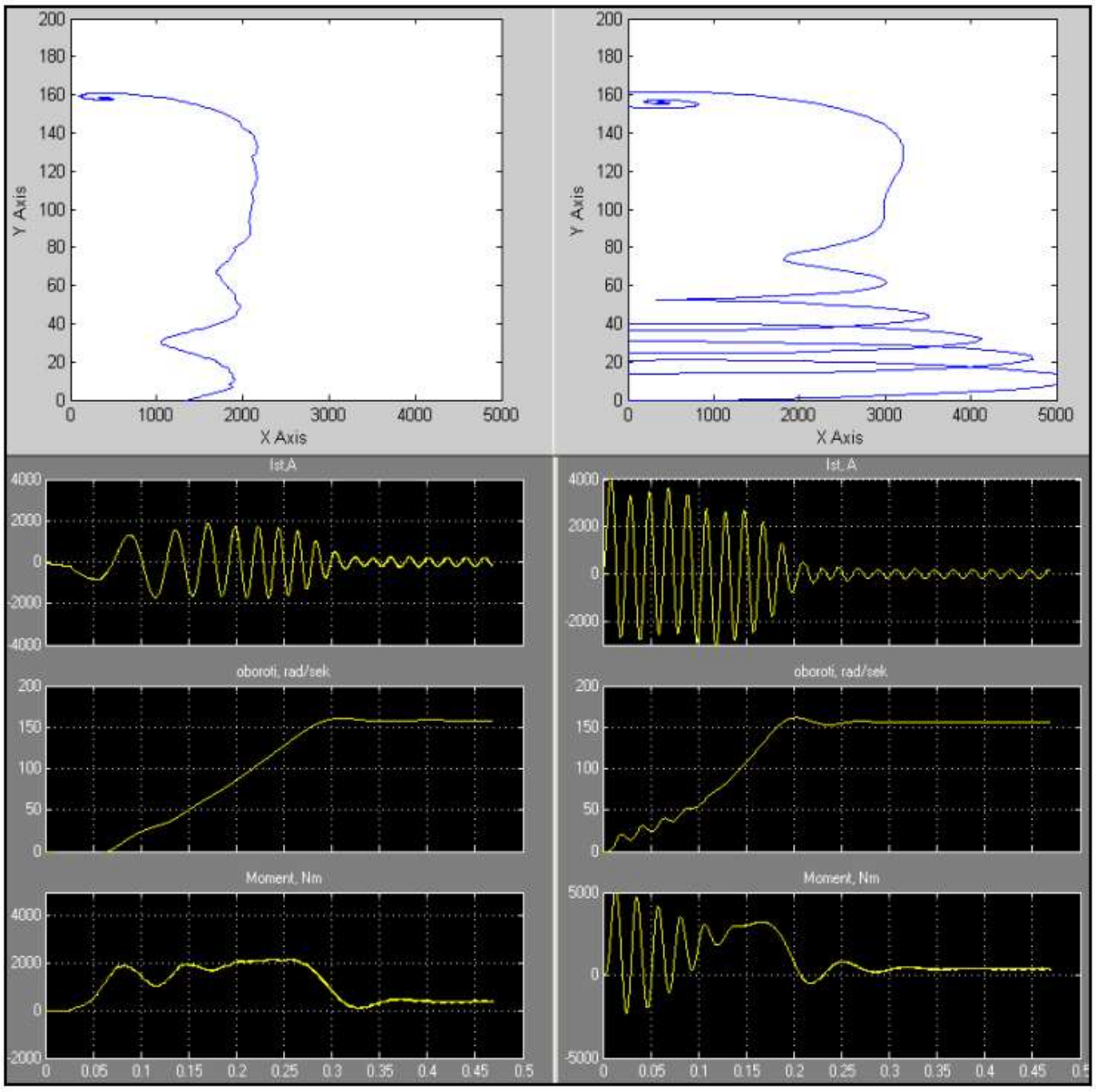


Figure 8. Comparison diagrams of starting a KU engine with a frequency control system and a traditional control system

Let us introduce the concept of the acceleration coefficient (β). This coefficient determines the slope of the linear frequency increase with respect to the time axis (Figure 9). The larger it is, the larger the amplitude of the transition parameters.

a conventional K Q starting system, β = 90°. Similar to the transients of electronic circuits, the maximum transient currents and voltages occur at the sharp leading edge of the input waveform, just as in AD with frequency acceleration. By this analogy, the duration of the motor starting transient is: $T_{transition}$ =3…5τ

$\tau = \frac{L}{R}$(9)

here:

τ– time constant, s;

L– inductance of the motor stator winding, H;

R– Active resistance of the AD stator winding, Ω.

For the 5AH315A2C engine, the duration of the transition process is $T_{transition}$ = 0.369 s, if β= 1

Acceleration coefficient β It is convenient to relate to the duration of the transition process:$\beta = \frac{t_b}{T_{o'tish}}$

For example, in a conventional start-up, the supply frequency of 50 Hz is already set at 0 seconds of start-up, so that the coefficient β= 0

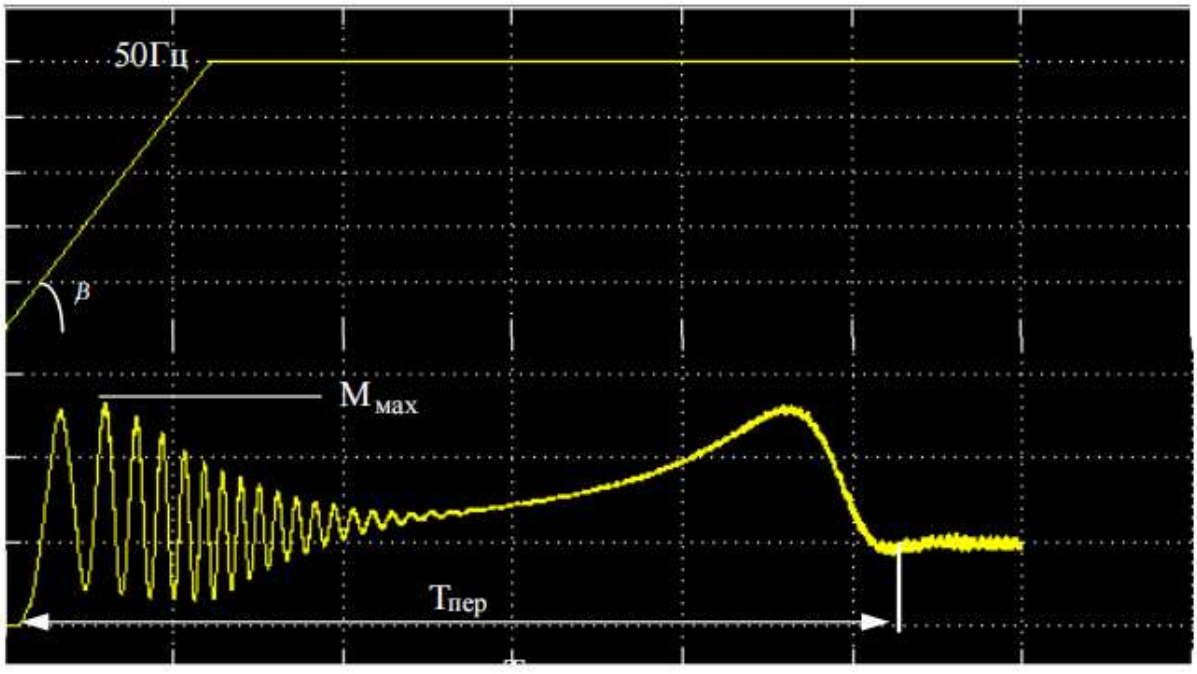


Figure 9. Diagram explaining the acceleration parameters when starting a K Q engine

Now let's look at the diagrams of starting characteristics with different acceleration coefficients (Table 3) and select the optimal acceleration mode for the 5AH315A2C engine.

Basic launch conditions:

Load torque – 400 Nm

Operating frequency – 50 Hz

Table 3. Comparison of acceleration coefficient and startup parameters

Acceleration coefficient	Maximum starting current, I, A	Max/Min starting torque, critical torque, Nm	Duration of the transition process, T_transition, s
3.5	700	750/650, 650	-
2.5	1000	1000/500, 790	1,125
1.25	1400	1100/400, 1300	0.69
1	1800	1200/350, 1300	0.65
0.815	1850	1250/300, 1300	0.68

Acceleration coefficient	Maximum starting current, I, A	Max/Min starting torque, critical torque, Nm	Duration of the transition process, T_transition, s
0.520	1900	1280/250, 1300	0.71
0.5	1950	1400/100, 1300	0.74
0.38	1950	1580/-50, 1300	0.76
0.35	1950	1600/-150, 1300	0.78
0.31	1950	1600/-200, 1300	0.8
0.26	1950	1750/-400, 1300	0.82
0.25	1950	1800/-500, 1300	0.825
0.185	1950	1800/-550, 1300	0.83
0.125	1950	2000/-600, 1300	0.84
0.1	1950	1900/-700, 1300	0.85
0	1950	1800/-800, 1300	0.85

According to the research results, 14 starting characteristics are included in Table 3. As can be seen from the table values, if the acceleration coefficient is greater than the analytically calculated transition period, the real transition period increases and the starting current approaches the nominal value:

$$\beta > T_{o\prime tish.his} \rightarrow T_{o\prime tish.real} \uparrow, I_{IT} \downarrow, M \approx M_{kr} \approx M_{IT}$$

With a sufficiently high acceleration coefficient, the transient values of the current are smoothed out. The amplitude of the current increases by a factor of 1.5–2, but this start-up occurs for a few seconds, so for the K Q system it is insignificant.

If the acceleration coefficient is less than the calculated transition time, the starting current remains at its maximum value, the duration of the transition process increases, and the starting torque increases:

$$\beta \leq T_{o\prime tish.his} \rightarrow T_{o\prime tish.real} \uparrow, I_{IT} = const, M_{IT} \uparrow$$

As the acceleration coefficient decreases further, a negative starting torque appears and the starting torque drops below zero, which negatively affects the characteristics of the AD.

The analysis conducted shows that the optimal acceleration coefficient is based on the following criteria:

$$\begin{cases} M_{kr} = const; \\ M_{IT} \to min \cup M_{IT} \geq 0; \\ I_{IT} \to min; \\ T_{o'tish} \to min \end{cases}$$

proposes to replace the traditional control systems of the drive motors of the compressor unit with a frequency control system. For this purpose, the algorithm for forming the control signal and the frequency control law are selected in the work. On this basis, a mathematical model of the control effect is developed.

To demonstrate the performance of the method, a simulation model of the drive motor control of the 5AH315A2C compressor unit was developed. The model boundaries were determined from the obtained diagrams and the appropriate coefficients were selected.

In addition, the work conducted an experimental experiment on the parallel operation of two models: a conventional control system and a motor system with frequency control. The main characteristics of both methods were measured and a comparative analysis was conducted. As a result, the obvious advantages of the frequency method were identified.

It is also determined that the transition parameters in frequency starting depend on the engine acceleration. For this purpose, the concept of acceleration coefficient is introduced and a criterion for its optimal value is established. Under these conditions, the minimum of electrical and time parameters in the transition, as well as smoother engine control, is ensured.

References

1. Атамирзаев, Т. У., Зокирова, Д. Н., Абдусатторов, Н. Н., & Исмоилов, Х. А. (2019). Энергосбережения при внедрении в производство асинхронных

двигателей с совмещёнными обмотками (адсо). *Экономика и социум*, (3 (58)), 125-128.

2. Атамирзаев, Т. У., & Зокирова, Д. Н. (2019). Modern technologies and devices with use of secondary energy sources in uzbekistan and in the world. *Научное знание современности*, (2), 39-43.

3. Otamirzaev, O. U., Zokirova, D. N. M., & Sharipov, F. F. (2019). USE OF ENERGY SAVING CABLES IN ELECTRIC ENERGY TRANSFER. *Научное знание современности*, (3), 92-96.

4. Zokirova, D. N., & Sh, T. U. (2023). AVARIYA REJIMIDA ENERGIYA TIZIMINING O'TKINCHI JARAYONLARINI MATLAB SIMULINKDA TADQIQ QILISH. *Экономика и социум*, (5-2 (108)), 502-508.

5. Юсупов, О. Я., Зокирова, Д. Н., Тойчиева, М. О., & Мухиддинова, Ф. Б. (2019). Методы и средства контроля показателей качества электрической энергии. *Экономика и социум*, (3 (58)), 512-515.

6. Nematillaevna, Z. D. (2024). APPLICATION OF ENERGY-SAVING DISTRIBUTION TRANSFORMERS IN INDUSTRIAL ENTERPRISES. *Ethiopian International Journal of Multidisciplinary Research*, *11*(12), 26-30.

7. Зокирова, Д. Н., Қурбонова, Ф. Қ., & Хусаинов, Ж. И. Ў. (2022). ҚУРИТГИЧЛАРДА ҚУРИТИЛАДИГАН МЕВАЛАРНИНГ ГИГРОСКОПИК ВА ТЕРМОРАДИАЦИОН ХАРАКТЕРИСТИКАЛАРИНИ ТАДҚИҚ ЭТИШ. *Academic research in educational sciences*, *3*(3), 392-400.

8. Zokirova, D. N., & Qosimov, M. U. (2023). SANOAT KORXONALARINI ELEKTR BILAN TA'MINLASH UCHUN ENERGIYA TEJAMKOR TAQSIMLOVCHI TRANSFORMATORLARNI TAHLIL QILISH. *Экономика и социум*, (5-2 (108)), 513-518.

9. Nematillaevna, Z. D. (2021). Problems in providing independent learning education and ways to prevent them. *Academicia: An International Multidisciplinary Research Journal*, *11*(1), 1431-1436.

10. Usubovich, O. O., & Ne'matillaevna, Z. D. (2022). Methodology of using connecting elements of science in the organization of independent work of the science of hydroelectric power stations.

11. Usubovich, O. O., & Nematillaevna, Z. D. (2022). Problems arising from the use of the case-study method and methods of Their Prevention. *Central Asian journal of social sciences and history*, *3*(6), 5-10.

12. Otamirzaev, O. U., & Zokirova, D. N. (2019). PROBLEMS ARISING WHEN APPLYING THE “BOOMERANG” METHOD IN THE COURSE OF TRAINING AND METHODS FOR THEIR ELIMINATION. *Scientific Bulletin of Namangan State University*, *1*(11), 270-274.

13. Usubovich, O. O., & Ne’matillaevna, Z. D. (2022). INTERFAOL USULLARDAN FOYDALANIB TALABALARNING MUSTAQIL FIKRLASHLARINI SHAKLLANTIRISH. In *E Conference Zone* (pp. 101-105).

14. Бекваевич, У. Қ., Отамирзаев, О. У., & Зокирова, Д. Н. (2022). The use of Interactive Methods in the Formation of Independent Thinking of Students and Their Analysis.

15. Отамирзаев, О. У., & Зокирова, Д. Н. (2014). Мустақил фикрлашларни шакллантиришга йўналтирилган дарс ишланмаси.

16. Химматалиев, Д. О., & Зокирова, Д. Н. (2022). НАЗАРИЙ ЭЛЕКТРОТЕХНИКА ФАНИНИ ТАЪЛИМ ТЕХНОЛОГИЯЛАРИ ТАРКИБИ АСОСИДА РЕЖАЛАШТИРИШ ВА УЛАРДАН ФОЙДАЛАНИШ. *Евразийский журнал академических исследований*, *2*(3), 630-638.

17. D.N.Zokirova , & Sh.Sh.Ahmadjanov (2026). Shamol g‘ildiragi tomonidan shamol oqimi energiyasidan foydalanishni nazariy tadqiq etish. Строительство и образование, 5 (2), 339-352.

18. D.N.Zokirova (2025). Nasos stantsiyalarida suv va energiya resurslaridan foydalanish samaradorligini oshirish. Строительство и образование, 4 (2), 466-475.

19. Zokirova D.N (2025). Nasos stansiyasidagi elektr qurilmalarning ish rejimlarini optimallashtirish. Ilm, tadqiqot va taraqqiyot / Наука, исследования и развитие, 5